# Chapter 12
# The High-Impact Weather Assessment Toolkit

**Patrick N. Gatlin, Jonathan L. Case, Jayanthi Srikishen, and Bhupesh Adhikary**

## 12.1 Introduction

Of the various types of weather phenomena, thunderstorms produce some of the most immediate and impactful hazards—damaging winds and hail, frequent lightning, and intense rainfall. Resilience to high-impact weather can be attained through investment in several key areas: proper infrastructure; effective emergency management; public education; and well-informed weather forecasting services. Unfortunately, some of the most intense thunderstorms occur in developing nations that have yet to build sufficient resilience to such weather hazards. Although there is a perceived cost associated with establishing National Hydrological and Meteorological Services (NHMS), investment in these services can boost the socioeconomic well-being of a developing nation (e.g., Nepal) by a factor of 10 (Perrels 2011). Early warning services are identified as providing the greatest and most immediate socioeconomic benefit amongst other types of disaster risk reduction strategies (Hallegatte 2012).

The Hindu-Kush Himalaya (HKH) region is host to some of the most intense thunderstorms on Earth (Zipser et al. 2006), primarily during the pre-monsoon season (Cecil and Blankenship 2012), and is routinely plagued by the hazards they pose (e.g., Das et al. 2014; Bikos et al. 2015; NIRAPAD 2018). Their impact is

P. N. Gatlin (✉)
NASA Marshall Space Flight Center, Huntsville, AL, USA
e-mail: patrick.gatlin@nasa.gov

J. L. Case
ENSCO, Inc, Huntsville, AL, USA

J. Srikishen
Universities Space Research Association, Huntsville, AL, USA

B. Adhikary
International Centre for Integrated Mountain Development, Kathmandu, Nepal



B. Bajracharya et al. (eds.), *Earth Observation Science and Applications for Risk Reduction and Enhanced Resilience in Hindu Kush Himalaya Region*,
https://doi.org/10.1007/978-3-030-73569-2_12

especially felt in Bangladesh where many documented tornado events have caused hundreds of fatalities, including over 700 in one event in April of 1996, and at least 1300 in a single event on 26 April 1989 (Bikos et al. 2015). A recent notable thunderstorm event in Bangladesh occurred on 30 March 2018, causing 282 casualties (at least six of them fatal), damaging 943 houses, and destroying large swaths of crops as a result of a tornado and other strong winds and large hailstones (222 of the casualties solely due to hailstones; NIRAPAD 2018). Furthermore, lightning vulnerability has become more prominent in Bangladesh with more than 250 fatalities recorded per year from 2010 to 2016 (Dewan et al. 2017). And, recent storm events on 29–30 April 2018 and 9–10 May 2018 produced widespread frequent lightning that resulted in 74 fatalities in Bangladesh.

Even though Nepal is less densely populated than Bangladesh, it has also suffered damages due to similar weather hazards (Fig. 12.1). On 31 March 2019, the first-ever documented tornado occurred in southern Nepal, leading to 30 deaths, 1150 casualties, and destroying 2890 homes (Mallapaty 2019; Shrestha et al. 2019). [It is likely that tornadoes occur in Nepal on a more regular basis during the pre-monsoon season but have historically gone undocumented due to the lower population density and lack of effective communication tools]. More prominent in Nepal have been hailstorms, such as the event in 2006 that caused crop and livestock damages which exacerbated local food shortages (ACTI 2006).

Although many NHMS in developing regions such as the HKH have access to weather forecasting tools, they currently lack the information required to support early warning services and timely disaster response that can help mitigate the impacts of hazards that are produced by frequent and intense thunderstorms. As these services undergo modernization efforts, which include enhancements in

**Fig. 12.1** Weather hazard is a major issue in the mountains during monsoon seasons. Photo by Santosh Raj Pathak

observational infrastructure (e.g., Rigaud 2015; World Bank Group-PPCR 2015; World Bank 2017), investments in new computational tools that will support enhanced early warning services are also necessary.

## 12.2 Forecasting High-Impact Weather

Numerical weather prediction (NWP) is the primary tool used by NHMS to produce weather forecasts. In particular, the Weather Research and Forecasting (WRF) model (Powers et al. 2017) has become the most widely used regional forecast and simulation tool in the weather community (e.g., Kain et al. 2006; Tao et al. 2016; Schwartz et al. 2019), including by NHMS in the HKH region (e.g. Ahasan et al. 2014; Kotal et al. 2015). Operationally, the WRF model is typically configured to provide hourly regional weather forecast guidance up to three or four days. Although WRF is a powerful tool, it still cannot replace a sufficiently dense observational network when it comes to monitoring and nowcasting (i.e., 0–1 h forecasts) rapidly unfolding weather such as thunderstorms. However, in countries such as Nepal such observations are often limited due to the terrain or lack of investment in Doppler weather radar networks that are critical to assessing such high-impact storms. Thus, it is critical that NHMS possess highly relevant and skillful NWP to gain proper situational awareness of potential weather hazards during the forecast period.

### *12.2.1 Challenges of Forecasting Thunderstorms*

Regional models such as WRF also require input from the global NWP in order to represent the initial state and evolution of the atmosphere on a larger scale that can orchestrate high-impact weather events through their interaction with land and ocean. Hence, it is important to properly represent the initial state of the land–atmosphere–ocean system for regional modeling applications, which entails bringing observations into the NWP framework via data assimilation methods. Since in situ observations are rather limited across the globe, NWP in such regions often incorporates the geophysical variables retrieved via satellite-based remote sensing into data assimilation algorithms using radiative transfer models to relate satellite observations to NWP model state variables (Barker et al. 2012; Geer et al. 2017). However, satellite retrievals are not straightforward and introduce additional uncertainty in the model initial conditions. Furthermore, there are a variety of data assimilation techniques, some of which can provide significant improvements to the forecast (e.g., Huang et al. 2009), but they can be rather complex and computationally expensive, especially for real-time applications.

Proper forecast of thunderstorm hazards requires the use of a convection-permitting model (i.e., its horizontal grid spacing must be on the scale of 4–5 km or

finer). This model must adequately depict all physical processes and interactions between the land/ocean and atmosphere that lead to cloud and precipitation development and decay. Since explicitly simulating all of these interactions and processes is not feasible, they must be parameterized (i.e., approximated) within the model (Stensrud 2007). Convection-permitting (also referred to as cloud-resolving) models often include parameterizations of sub-grid-scale motions (e.g., turbulent motions within the boundary layer), mixed-phase microphysics, and radiative processes (Guichard and Couvreux 2017). Decades of research have gone into developing cloud-resolving models and parameterizations of these physical processes (Tao 2007). As a result, numerous parameterization schemes have been incorporated into the Advanced Research WRF for simulating thunderstorms (UCAR 2020). This is promising for improving the skill of model forecasts, but it requires choosing the appropriate ones for the application at hand. There have been a multitude of sensitivity tests of parameterization schemes (e.g., Milbrandt and Yau 2006; Cohen et al. 2015; Fan et al. 2017), but no single combination of parameterizations works best for all thunderstorm hazards, weather regimes, and geographical regions.

### *12.2.2 Ensemble-Based, Convection-Allowing NWP*

In light of this wide variety of potential configurations, model uncertainty, and differing assumptions within individual parameterizations, a solution has been to perform ensemble NWP by running a suite of different model runs. Each model run may be configured with a different combination of parameterizations and/or initial conditions. The main idea of ensemble NWP is to capture the range of possible solutions (e.g., Fig. 12.2), and thereby enable probabilistic-based forecast information that facilitates a more well-informed decision. To improve thunderstorm forecasts in the United States, regional WRF-based convection-allowing models (e.g., Kain et al. 2006, 2010) have been used in an ensemble configuration (e.g., Clark et al. 2012; Schwartz et al. 2019) to support severe weather and excessive precipitation forecast experiments in the National Oceanic and Atmospheric Administration (NOAA) annual Hazardous Weather Testbed's Experimental Forecast Program (Clark et al. 2012). This particular forecast system included over two dozen different model simulations that produced hourly forecasts out to 30 h at convection-allowing grid spacings (1–4 km) spanning the continental U.S. Similar experimental ensemble forecast demonstrations have been undertaken by the National Center for Atmospheric Research (NCAR) and have received much fanfare from the weather community (Schwartz et al. 2019), but their relatively large computational burden hinders their implementation by operational agencies with relatively limited resources.

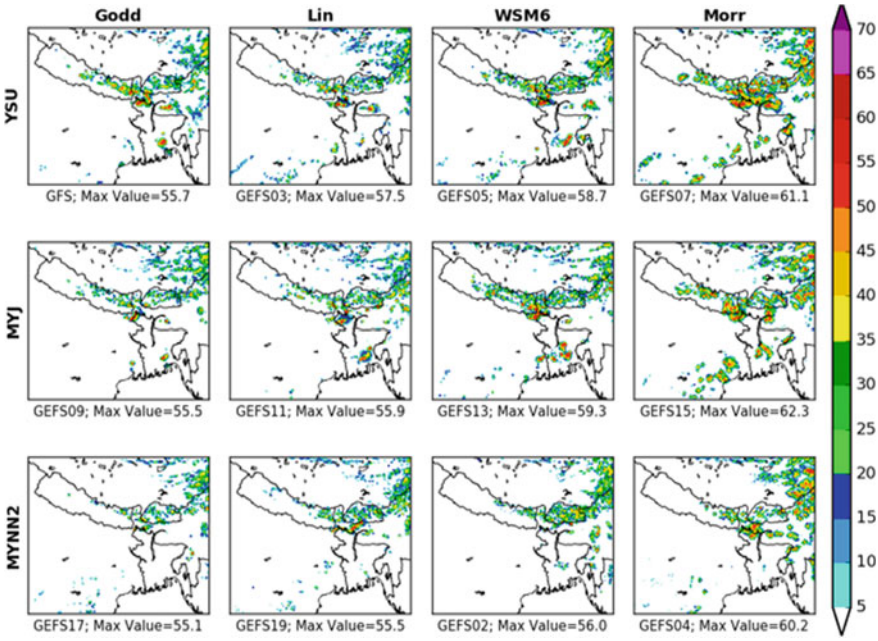


**Fig. 12.2** An example of the range of different weather scenarios produced at the same forecast hour. Shown is the composite reflectivity, a metric for gauging thunderstorm intensity, which was produced by the HIWAT ensemble WRF runs on 25 April 2019. Traditional approaches to operational NWP only provide a solution based on a single model run (e.g., top-left panel), which may not be the correct one given the uncertainty in the model-based representation of the atmosphere and its evolution. Hence, ensemble-based NWP provides a variety of solutions that can be combined to obtain the probability of a weather hazard at any point in the forecast cycle

## 12.3 A High-Impact Weather Service for the HKH Region

In response to the need to build the resilience of the HKH region to high-impact weather, NASA SERVIR developed a new tool for use by NHMS in the region. The High-Impact Weather Assessment Toolkit (HIWAT) is a service that provides probabilistic-based thunderstorm hazard forecast guidance to NHMS forecasters and other weather-sensitive decision makers. HIWAT uses a convection-allowing ensemble modeling system similar to that developed for experimental hazardous forecast demonstrations in the U.S. (e.g., Clark et al. 2012; Schwartz et al. 2019), but it is tailored for NHMS in the HKH region.

### 12.3.1 Model Configuration

The WRF model is configured in HIWAT using an outer domain with 12-km grid spacing centered on South Asia, a 4-km inner domain that includes Nepal, Bangladesh, Bhutan, and north-eastern India (Fig. 12.3), and 42 terrain-following vertical levels ranging from the ground to a barometric altitude of 20 hPa.

The larger 12-km domain is primarily used for regional synoptic-scale situational awareness and, more importantly, to downscale the boundary and initial conditions obtained from the larger global-scale model to the higher-resolution nested grid. The 12-km resolution outer domain parameterizes convection using the Kain-Fritsch scheme (Kain 2004). On the 4-km domain, the cumulus parameterization is turned off to explicitly simulate convective storms (i.e., convection-allowing). Although a higher resolution would likely result in a more accurate representation of the convective processes and subsequent thunderstorm intensity (e.g., Potvin and Flora 2015), the resolution used in HIWAT is a trade-off between reducing the computational burden while retaining the capability to forecast the hazards posed by mesoscale weather systems (e.g., Weisman et al. 1997; Bryan and Morrison 2012).

For simulating thunderstorms, the representation of the planetary boundary layer (PBL) processes that lead to convective initiation and the microphysical processes that result in precipitation development are key. Hence, the HIWAT ensemble forecasting system has diversity in the parameterization of the PBL and microphysics (Table 12.1). Each of the microphysical schemes account for riming (i.e., formation of graupel/hail)—a critical process in the development of deep convective storms and lightning (see review by Williams 2001). To include additional

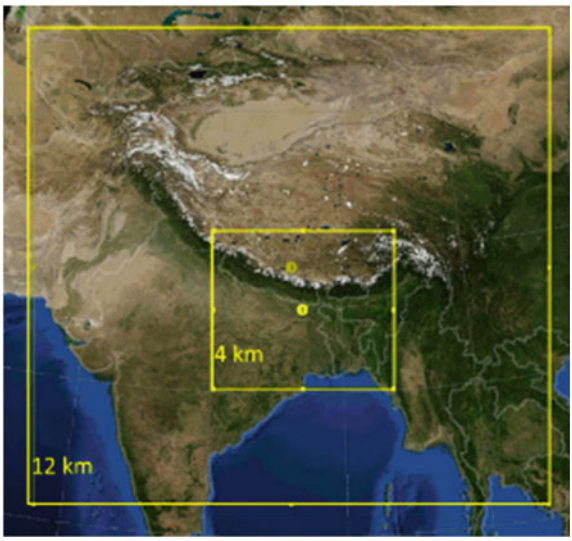


**Fig. 12.3** Map of HIWAT domains over Asia

**Table 12.1** Ensemble configuration of the 4-km resolution domain of the WRF-based probabilistic forecasting system used in HIWAT-HKH

| Key: *ensemble member* initial condition | | Microphysical parameterization | | | |
|---|---|---|---|---|---|
| | | Goddard (Tao et al. 2016) | Purdue Lin (Chen and Sun 2002) | WSM6 (Hong and Lim 2006) | Morrison 2-moment (Morrison et al. 2009) |
| PBL parameterization | YSU (Hong et al. 2006) | *HKH1*: GFS | *HKH2*: GEFS 03 | *HKH3*: GEFS 05 | *HKH4*: GEFS 07 |
| | MYJ (Janjić 1994) | *HKH5*: GEFS 09 | *HKH6*: GEFS 11 | *HKH7*: GEFS 13 | *HKH8*: GEFS 15 |
| | MYNN2 (Nakanishi and Niino 2009) | *HKH9*: GEFS 17 | *HKH10*: GEFS 19 | *HKH11*: GEFS 02 | *HKH12*: GEFS 04 |

The NCEP/EMC model used for initial/boundary conditions is listed beneath each named ensemble member

diversity and spread in the HIWAT ensemble, the initial conditions are varied. The operational run of the Global Forecast System (GFS; Zhou et al. 2019) and members from the Global Ensemble Forecast System (GEFS; e.g., Guan et al. 2015; Zhou et al. 2017), which are run every 6 h by the U.S. National Centers for Environmental Prediction (NCEP) Environmental Modeling Center's (EMC) and freely obtained from them, are used to initialize the WRF model employed by HIWAT. Also, HIWAT ingests a 2-km resolution, northern-hemispheric sea surface temperature (SST) composite product derived from NASA's MODIS and VIIRS satellite measurements (Zavodsky et al. 2017), which improves upon the considerably coarser SST analysis in the GFS/GEFS models. To execute the ensemble WRF model runs, HIWAT employs the Unified Environmental Modeling System (UEMS; Rozumalski 2019), which greatly simplifies the complex workflow involved in NWP by managing data acquisition, initialization, pre- and post-processing, and generating derived fields.

### *12.3.2 Probabilistic Forecast Products*

The primary guidance products generated by HIWAT are probabilistic forecasts of the thunderstorm hazards associated with tornadoes, damaging wind and hail, frequent lightning, and intense rainfall. These are provided at each hour of the forecast cycle and temporally composited into daily summary probability maps that can readily facilitate the convective outlooks of thunderstorm hazards (Fig. 12.4), which is a capability recommended in the report on the Bara-Parsa (Nepal) tornado of 31 March 2019 (Shrestha et al. 2019). Furthermore, products such as daily summaries provide a weather-sensitive decision maker the information in a concise

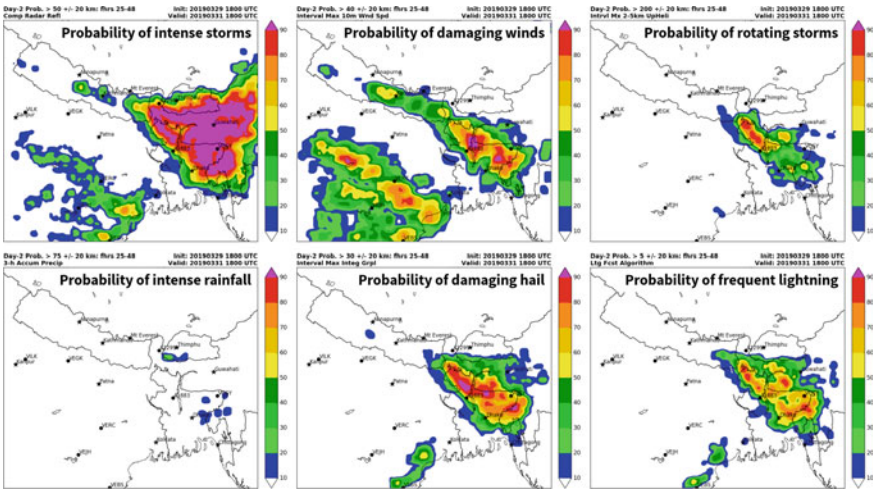


**Fig. 12.4** HIWAT probabilistic forecast of thunderstorm-related weather hazards for the Day-2 time period. Intense storms are defined as composite reflectivity exceeding 50 dBZ. Damaging winds are defined as the maximum 10-m wind speed in the previous hour (Kain et al. 2010) exceeding 40 kts. Rotating storms are defined as the maximum 2–5 km updraft helicity (Kain et al. 2008) in the previous hour exceeding 200 $m^2s^{-2}$. Intense rainfall is defined as the 3-hour accumulated precipitation exceeding 75 mm. Damaging hail is defined as the maximum column-integrated graupel in the previous hour (Kain et al. 2010) exceeding 30 kg $m^{-2}$. Frequent lightning is defined as one lightning flash per minute produced by the diagnostic WRF Lightning Forecast Algorithm (McCaul et al. 2009, 2020)

manner to quickly assess future thunderstorm impact(s). Because of uncertainties in model forecast accuracy, combined with convective features that typically have relatively small footprints (e.g., Kain et al. 2010), a 20-km spatial neighborhood (i.e., grid points within 20 km) is first applied to the individual ensemble member thunderstorm hazard fields prior to computing the probabilities. Additionally, a Gaussian smoother is used to produce smoother and more visually appealing probability maps. Such neighborhood approaches can result in more skillful probabilistic forecasts (Schwartz and Sobash 2017).

An example of the Day-2 summary forecast from HIWAT (i.e., a 25–48 h forecast period) is shown in Fig. 12.4. This gives the probability of the indicated weather hazard within 20 km of a point at any time of the Day-2 forecast period. Using composite reflectivity exceeding 50 dBz as a proxy for storms with significant precipitation rates (i.e., intense storms), we see there is greater than a 90% probability of intense storms occurring from southeastern Nepal across northern and eastern Bangladesh into southern Bhutan and Northeast India. A Day-2 convective outlook would highlight this region. The next question is the likelihood of specific hazards within this region. We see intense rainfall that might lead to flash-flooding should not be a major concern, but there are greater probabilities of damaging winds, hail, rotating storms, and frequent lightning across this region of intense

storms. Furthermore, the higher probability of rotating storms in northern Bangladesh being aligned with the relatively enhanced probability of damaging wind and hail suggest that tornadoes are more probable in northern Bangladesh than in eastern Bangladesh. This analysis of Fig. 12.4 is akin to the forecast process used by NOAA's Storm Prediction Center in the U.S. to determine future convective hazards (Jirak et al. 2014).

## 12.4 HIWAT Forecast Demonstrations

Two forecast demonstrations of HIWAT took place during the pre-monsoon (March-May) and monsoon seasons (June–August) of 2018 and 2019, with the Bangladesh Meteorological Department (BMD) and Nepal's Department of Hydrology and Meteorology (DHM). For these demonstrations, HIWAT used the public release of WRF version 3.7.1 (included in UEMS version 15.99.1), while NASA's SERVIR program provided the virtual computing cluster needed to run it. This virtual cluster consisted of 13 nodes, each with 16 dual-core Intel Xenon 2.10 GHz processors and 128 GB of RAM. It produced 0–48 h HIWAT-HKH forecast products within 6 h of HIWAT initialization. This resulted in a probabilistic forecast guidance covering two diurnal maximums in the convective activity in the HKH region (e.g., Romatschke et al. 2010; Mäkelä et al. 2014; Dewan et al. 2018).

During these demonstrations, HIWAT trainings were held in Kathmandu and Dhaka to familiarize the operational forecasters at DHM and BMD with HIWAT and its probabilistic-based thunderstorm hazard forecasting products. The products were made available to forecasters via two web-based display tools. An image viewer, which was contributed and hosted by NASA's Short-term Prediction Research and Transition Center (SPoRT; Jedlovec 2013), provided quick looks and animations of all current and archived HIWAT forecast products. Also, select HIWAT products were packaged (i.e., separate from the full model output suite) into a netCDF format for an interactive (i.e., pan, zoom, query) web-based application, which was produced within the Tethys platform (Nelson et al. 2019), to enable efficient interrogation of the forecasts within a web-mapping service. The Tethys-based HIWAT Model Viewer App (Fig. 12.5) provides users with the capability to quickly determine where, when, and how likely a thunderstorm hazard may occur. It also has the capability to provide the spatiotemporal statistics of a forecast variable (e.g., as to when maximum rainfall will occur within the selected area). Figure 12.5 shows the HIWAT forecast run from 29 March 2018 which indicates that a high-impact weather event is possible across the northern half of Bangladesh. The time-series plots of the forecast across this area show a greater than 60% chance of rotating thunderstorms, with a 45–55% chance of damaging winds and hail at the selected points between 11:00 and 15:00 UTC on 30 March 2018.

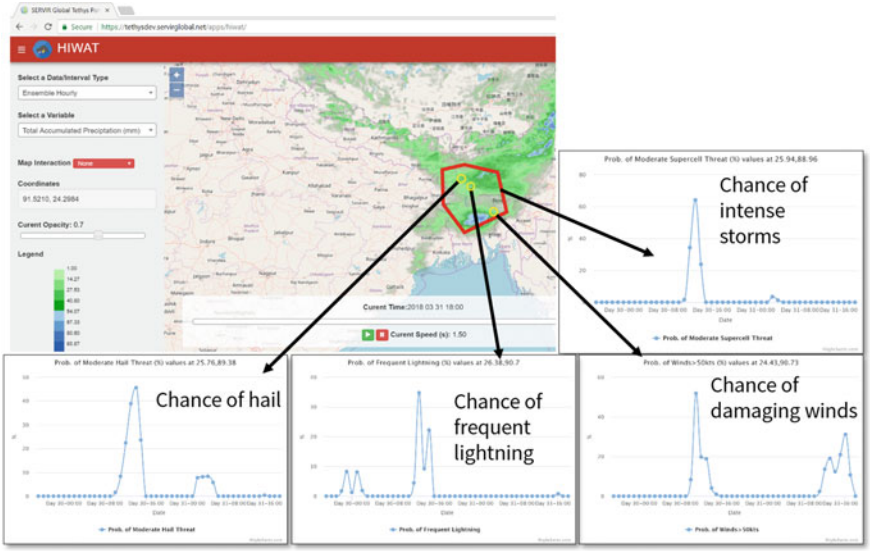


**Fig. 12.5** The Tethys-based HIWAT model viewer app

### *12.4.1 Hailstorm: 30 March 2018*

The severe thunderstorms that occurred across the eastern HKH on 30 March 2018 caused significant damages in Nepal, Bangladesh, and Northeast India (Fig. 12.6). In Bangladesh alone, over 274 casualties, numerous acres of crops, and several hundred houses were damaged, mostly due to large hail but also due to strong winds, and a tornado in Nepal's south-central districts of Bara and Parsa (Shrestha et al. 2019). The Day-1 probabilistic forecasts from the HIWAT-HKH runs, initialized at 18:00 UTC on 29 March 2018, are shown in Fig. 12.6a–c. They clearly indicate more than an 80% chance of hailstorms in northern and central Bangladesh and Meghalaya in north-east India (Fig. 12.6a). The forecast hotspots of frequent lightning overlap with this region (Fig. 12.6b), but they also extend further east, including Assam in Northeast India and Sylhet division in northeastern Bangladesh. It also shows a greater than 80–90% chance of 10-m AGL winds exceeding 50 kts ($\sim$93 km h$^{-1}$) in Sylhet (Fig. 12.6c).

Direct, near real-time observations of storm intensity are sparse in the rural areas of the HKH region; hence, HIWAT also consists of a satellite-based observational component to facilitate assessment of its forecasts. On 30 March 2018, at around 08:11 UTC, there was an overpass of the HKH region by the GPM Microwave Imager (GMI) onboard the GPM core satellite (Skofronik-Jackson et al. 2017). Passive microwave observations provided a measure of storm intensity through their sensitivity to the upwelling radiation at 37 GHz being scattered by precipitating ice such as hail (Spencer et al. 1987; Cecil 2009). Applying the empirical fits

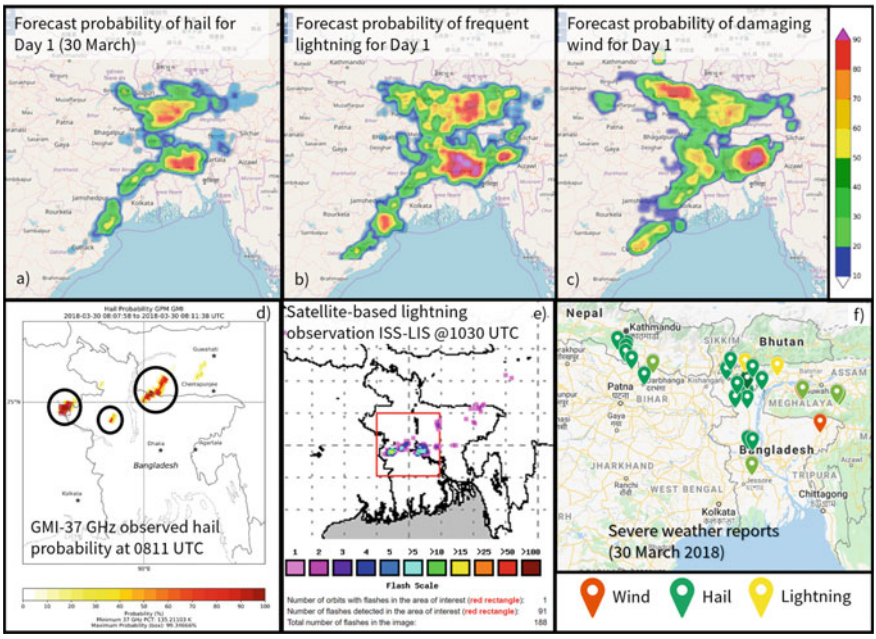


**Fig. 12.6** Performance of the HIWAT forecasts for the 30 March 2018 high impact weather event. **a–c** The 29 March 2018 forecasts from HIWAT-HKH indicate that thunderstorm-related hazards are highly likely to occur across parts of the eastern HKH on 30 March 2018. **d**, **e** Precipitation and lightning observations from the GPM core satellite radiometer and Lightning Imaging Sensor onboard the International Space Station, respectively, during overpasses of the eastern HKH region on 30 March 2018. **f** Location of damaging wind, hail, and lightning due to a high impact weather event in the eastern HKH region on 30 March 2018

of Bang and Cecil (2019) that relate the polarization-corrected brightness temperature at 37 GHz to the probability of hail observed at the ground, the GMI observations indicated three intense storms over the region with a greater than 75–95% chance of producing damaging hail at the ground, especially in north-western Bangladesh and west of Cherrapunjee, India (Fig. 12.6d). Similar damaging hail probabilities had been found for these storms with measurements from the Advanced Microwave Scanning Radiometer 2 (AMSR2) during its overpass about 30 min earlier (not shown). These patterns aligned with the northern-most local maxima of the hail probability forecast by HIWAT (Fig. 12.6a). Also, observations collected with the Lightning Imaging Sensor onboard the International Space Station (ISS) (Blakeslee et al. 2020) during an overpass at 10:30 UTC depict three individual thunderstorms with relatively higher lightning flash activity over central Bangladesh where the HIWAT forecasts suggested nearly a 100% chance of frequent lightning (Fig. 12.6e). Finally, the reports of thunderstorm-related damage, although likely incomplete and affected by subjective reporting, largely corroborated the HIWAT Day-1 forecasts that strongly suggested a high-impact weather

event unfolding from eastern Nepal to Northeast India and central Bangladesh (Fig. 12.6f).

### 12.4.2 Lightning

Lightning-related casualties have increased in Bangladesh in recent years (Dewan et al. 2017; Holle et al. 2018), so much so that the government declared lightning as a national disaster in 2016. During the 2018 pre-monsoon season, there were 275 reported casualties (215 of them fatal) due to lightning in Bangladesh, with 181 of these occurring during a two-week period in late April and early May (Fig. 12.7a). Although agricultural practices in Bangladesh during the annual peak lightning months of April and May contribute to the vulnerabilities (Dewan et al. 2017; Holle et al. 2019), a lack of capacity to forecast lightning is also a factor.

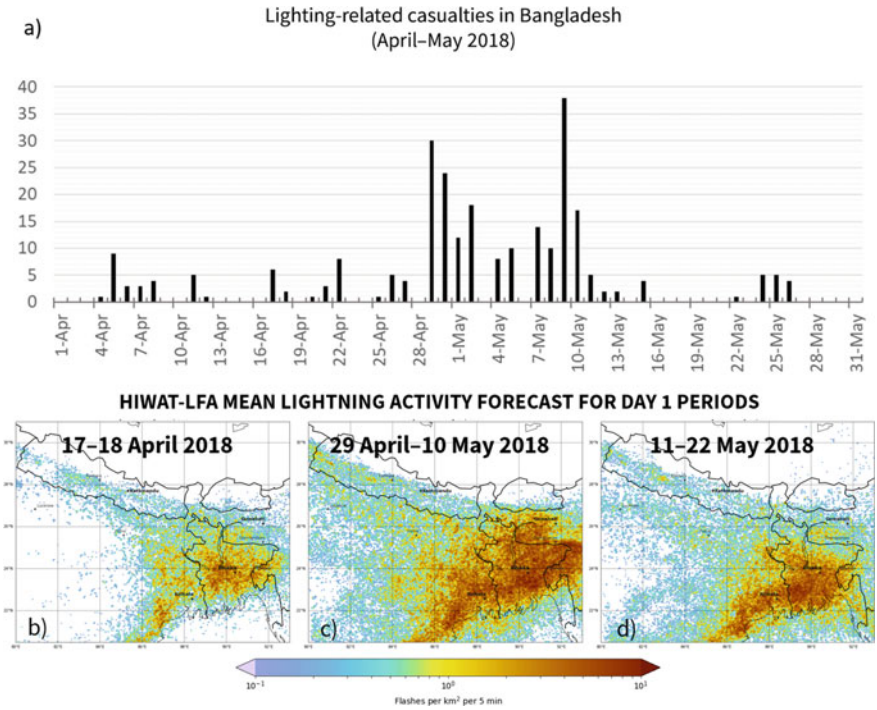


**Fig. 12.7** Impact of lightning activity on Bangladesh and select forecasts from HIWAT-HKH during April and May 2018. **a** Lightning-related casualties reported in Bangladesh between April and May 2018 (*Source* NIRAPAD 2018). **b–d** The mean 24-hour (i.e., Day-1) forecast flash rate density from the HIWAT-HKH ensemble for three different periods centered on the peak number of lightning-related casualties in panel a

One of the tools used in HIWAT is the Lightning Forecast Algorithm (LFA), which uses the convection-allowing WRF-simulated fields important to the storm electrification process as inputs, and computes a calibrated total lightning (both cloud-to-ground and cloud flashes) flash rate density (McCaul et al. 2009, 2020). This total lightning prognostic field is produced for each of the HIWAT ensemble members to produce the hourly and daily probabilistic lightning forecasts across the model domain (e.g., Figs. 12.5 and 12.6). Figure 12.7b–d provides a daily summary of the HIWAT lightning forecasts from 17 April to 22 May 2018. The amount of lightning being forecast increases from mid-April to early May, then decreases by mid-May, especially across northeastern Bangladesh and Northeast India. This trend compares very well with the trend in lightning casualties reported in Bangladesh during this time period (Fig. 12.7a). Also, Holle et al. (2019) found that the farming districts in northeastern Bangladesh are especially susceptible to lighting-related fatalities during April and May. Lightning safety education, especially related to agricultural practices (e.g., best times of day to tend or harvest crops), can greatly help reduce the adverse impacts of thunderstorms in the region. However, it is not every day that thunderstorms will occur in the same location at the same time, and it is not practical to halt work every afternoon during the peak harvesting months (April and May) of Boro rice, potato, and wheat. Hence, access to more informative weather forecasts such as those provided by HIWAT can facilitate better planning of day-to-day activities.

### *12.4.3 High-Intensity Rainfall Forecasting*

Another reason for using ensemble NWP is to enable the forecasting of flash floods in the regions affected by localized, intense rainfall associated with thunderstorms (Fig. 12.1). In an ensemble system such as HIWAT, hydrologists can access the information provided by the system's multiple precipitation forecasts in such a manner to concisely convey the expected outcome with a higher degree of confidence. This can be in the form of probabilities of rainfall exceeding some threshold in a given basin, which may not be readily known, or in the form of an envelope of streamflow forecasts for each basin. Most streamflow models require a single deterministic input of precipitation instead of a probability of precipitation. However, simply averaging the precipitation forecasts of each ensemble member will simultaneously over-predict the areal coverage of rainfall and reduce the amplitude of more intense rainfall events that are often the cause of the flash flooding in the smaller basins and urban areas. Hence, HIWAT employs a statistical technique known as the probability matched mean (PMM; Clark 2017) to provide a single precipitation forecast that represents a "most probable solution" from all its ensemble forecast members. The PMM not only retains the higher-amplitude precipitation intensity from the individual ensemble members but also retains the more spatially accurate pattern of the ensemble mean, with the bias at any precipitation threshold being about the same as the average bias of the

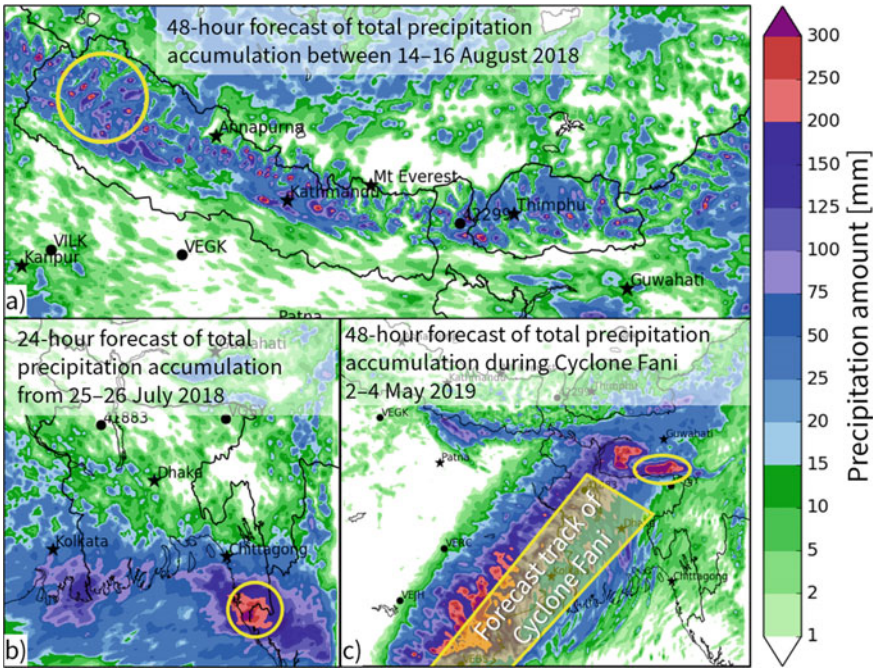


**Fig. 12.8** Examples of HIWAT-HKH ensemble precipitation forecasts using the PMM method. The circled regions indicate areas where extreme rainfall was observed within a 1–2 day period, as discussed in the text

individual members (Ebert 2001; Clark 2017). The PMM precipitation product reaps the benefit of an ensemble forecast and also provides the accumulations required by hydrologic applications.

Although HIWAT-HKH is largely focused on severe storms that occur in the HKH region during the pre-monsoon season, the 2018 and 2019 demonstrations were expanded to the wet monsoon season (June –September) at the request of the end users (i.e., DHM and BMD) and primarily for the purpose of flash-flood forecasting. A few events from 2018 to 2019 are highlighted in Fig. 12.8 to demonstrate the utility of the HIWAT PMM forecasts of precipitation during heavy rainfall episodes. The top panel of Fig. 12.8 shows the PMM-based forecast of precipitation exceeding 200 mm in several highly localized areas within the Himalayan foothills and mountains. Flash flooding was reported in several small basins in western Nepal between 15 and 16 August 2018, including a particularly devastating one along the Jhupra River in Nalgad of Jajarkot district (The Kathmandu Post 2018). The bottom panels of Fig. 12.8 show other heavy rainfall events captured by HIWAT-HKH. On 25 July 2018, the HIWAT PMM-based forecast indicated precipitation accumulation would exceed 300 mm within a 24-h period in southeastern Bangladesh, near Cox's Bazar (Fig. 12.8b). The BMD's automated weather station in Cox's Bazar recorded a 24-h rainfall accumulation of

315 mm on 26 July 2018. The third example (Fig. 12.8c) is the 48-h PMM-based precipitation forecast of the tropical cyclone Fani, which developed in the Bay of Bengal and made its landfall southwest of Kolkata, India, on 2 May 2019. The spread of the 12-member ensemble runs indicated that after landfall, Fani would move north-east along the coastline and significantly weaken as it crossed into Bangladesh. Typically, cyclones bring a significant flooding threat to Bangladesh, but according to the HIWAT forecast Fani carried a low risk of flooding as the heaviest corridor of rainfall was forecast to stay west of Bangladesh and in the Northeast Indian state of Meghalaya. The 48-h forecast predicted over 250–300 mm of rainfall around Cherrapunjee in Northeast India (Fig. 12.8c), where an automated weather station recorded 276 mm of rainfall between 3 and 4 May 2018.

The HIWAT demonstrations during 2018 and 2019 also included a hydrologic component in which the PMM-based forecast precipitation accumulations were used as input to the model of Routing Application for Parallel computation of Discharge (RAPID; David et al. 2011) in order to produce streamflow forecasts for the HKH region (Nelson et al. 2019). The HIWAT forecasts were used in this system primarily for forecasting flash floods due to intense rainfall in the smaller basins that are often not captured by the coarser-resolution global weather forecast models.

## 12.5 Summary, Challenges, and Way Forward

A probabilistic weather forecasting system such as HIWAT demonstrates the importance of ensemble-based NWP in building resilience to high-impact weather in the HKH region. The wealth of information it provides can improve decision-making and enhance weather services. Extreme-weather forecasting is often plagued with uncertainty and cannot be captured nor effectively conveyed through a single weather model. However, a convection-allowing ensemble forecasting system depicts a range of possible scenarios of intense thunderstorm hazards and thereby can help convey the amount of confidence and/or uncertainty of these hazards in the forecast. In order to effectively carry this out, the ensemble has to be properly configured to address the weather phenomena, including the uncertainty in the physical understanding and representation of it. Additionally, the ensemble forecasts, which may include hundreds of potential visualization products, must be made easily digestible for the decision makers. Some of these products for assessing potential threats from severe weather events have been presented herein and others can be found in a review by Roberts et al. (2019).

A big challenge for NHMS, especially in the case of developing nations, is the computational resources that are required by the ensemble weather forecasting systems. The computational load depends upon the number of ensemble members, the number and geographical size of the modeling domains, their spatial resolution, and the designated number of forecast hours. The complexity of the forecast system (i.e., workflow) must also be considered. Additionally, reliable and high-speed

internet access is needed to obtain the global models that initialize and provide boundary conditions to regional forecast systems such as HIWAT. Another challenge for NHMS lies in the novelty of the ensemble NWP, especially as a tool for thunderstorm forecasting. Also, continued education on advancements in meteorological forecasting techniques are needed since many meteorologists in developing nations have not received formal training on probabilistic-based weather forecasting.

The HIWAT service was designed with these challenges in mind. Although the HIWAT demonstrations consist of 12 separate WRF runs, HIWAT is fully customizable (in terms of domain size, number of ensemble members, and forecast hours) to accommodate porting the service to other regions. Also, and just as important, the myriad outputs from the individual ensemble members are combined into a handful of meaningful products relevant to addressing high-impact weather. These products are designed to be efficiently interpreted and are used to effectively convey the probability of thunderstorm hazards. HIWAT has demonstrated to NHMS in the HKH region the capability to build or enhance its capacity to provide services related to extreme-weather events. However, local NHMS may need to collaborate with scientific researchers to further customize the toolkit using thresholds that are based on more geographically-specific observations. The default thresholds used in the HIWAT demonstrations are primarily based on investigations focused on severe weather in the U.S. Furthermore, while information on familiar meteorological variables such as temperature, humidity, pressure, and wind are available from many regional observation networks operating in developing nations, more detailed information is needed to assess the storm prediction fields provided by a system such as HIWAT. Weather radars, especially those with Doppler and polarimetric capabilities, and lightning detection networks can provide critical observational evidence to evaluate the performance of this type of convection-allowing modeling system as well as enable additional refinement of the toolkit. This process of obtaining appropriate data, analyzing it, and using it to fine-tune the system to address local needs underscores the need for governments to establish a collaboration between their NHMS and the research community, either locally or abroad.

## References

ACTI (2006) Nepal: winter drought and hailstorm cause hunger, p 1. http://reliefweb.int/report/nepal/nepal-winter-drought-and-hailstorm-cause-hunger

Ahasan MN, Quadir DA, Khan KA, Haque MS (2014) Simulation of a thunderstorm event over Bangladesh using WRF-ARW model. J Mech Eng 44:124–131

Bang SD, Cecil DJ (2019) Constructing a multifrequency passive microwave hail retrieval and climatology in the GPM domain. J Appl Meteorol Climatol. https://doi.org/10.1175/JAMC-D-19-0042.1

Barker D et al (2012) The weather research and forecasting model's community variational/ensemble data assimilation system: WRFDA. Bull Am Meteorol Soc 93:831–843. https://doi.org/10.1175/BAMS-D-11-00167.1

Bikos D, Finch J, Case JL (2015) The environment associated with significant tornadoes in Bangladesh. Atmos Res 167:183–195. https://doi.org/10.1016/j.atmosres.2015.08.002

Blakeslee RJ, Lang TJ, Koshak WJ, Buechler D, Gatlin P, Mach DM, Stano GT, Virts KS, Walker TD, Cecil DJ, Ellett W, Goodman SJ, Harrison S, Hawkins DL, Heumesser M, Lin H, Maskey M, Schultz CJ, Stewart M, Bateman M, Chanrion O, Christian H (2020) Three years of the lightning imaging sensor onboard the international space station: expanded global coverage and enhanced applications. J Geophys Res Atmos 125:e2020JD032918. https://doi.org/10.1029/2020JD032918

Bryan GH, Morrison H (2012) Sensitivity of a simulated squall line to horizontal resolution and parameterization of microphysics. Mon Weather Rev 140:202–225. https://doi.org/10.1175/MWR-D-11-00046.1

Cecil DJ (2009) Passive microwave brightness temperatures as proxies for hailstorms. J Appl Meteorol Climatol 48:1281–1286. https://doi.org/10.1175/2009JAMC2125.1

Cecil DJ, Blankenship CB (2012) Toward a global climatology of severe hailstorms as estimated by satellite passive microwave imagers. J Clim 25:687–703. https://doi.org/10.1175/JCLI-D-11-00130.1

Chen S-H, Sun W-Y (2002) A one-dimensional time dependent cloud model. J Meteorol Soc Japan Ser II 80:99–118. https://doi.org/10.2151/jmsj.80.99

Clark AJ (2017) Generation of ensemble mean precipitation forecasts from convection-allowing ensembles. Weather Forecast 32:1569–1583. https://doi.org/10.1175/WAF-D-16-0199.1

Clark AJ et al (2012) An overview of the 2010 hazardous weather test bed experimental forecast program spring experiment. Bull Am Meteorol Soc 93:55–74. https://doi.org/10.1175/bAms-d-11-00040.1

Cohen AE, Cavallo SM, Coniglio MC, Brooks HE (2015) A review of planetary boundary layer parameterization schemes and their sensitivity in simulating southeastern U.S. cold season severe weather environments. Weather Forecast 30:591–612. https://doi.org/10.1175/WAF-D-14-00105.1

Das S et al (2014) The SAARC STORM: a coordinated field experiment on severe thunderstorm observations and regional modeling over the South Asian region. Bull Am Meteorol Soc 95:603–617. https://doi.org/10.1175/BAMS-D-12-00237.1

David CH, Maidment DR, Niu G-Y, Yang Z-L, Habets F, Eijkhout V (2011) River network routing on the NHDPlus dataset. J Hydrometeorol 12:913–934. https://doi.org/10.1175/2011JHM1345.1

Dewan A, Hossain MF, Rahman MM, Yamane Y, Holle RL (2017) Recent lightning-related fatalities and injuries in Bangladesh. Weather Clim Soc 9:575–589. https://doi.org/10.1175/WCAS-D-16-0128.1

Dewan A, Ongee ET, Rahman MM, Mahmood R, Yamane Y (2018) Spatial and temporal analysis of a 17-year lightning climatology over Bangladesh with LIS data. Theor Appl Climatol 134:347–362. https://doi.org/10.1007/s00704-017-2278-3

Ebert EE (2001) Ability of a poor man's ensemble to predict the probability and distribution of precipitation. Mon Weather Rev 129:2461–2480. https://doi.org/10.1175/1520-0493(2001)129%3c2461:AOAPMS%3e2.0.CO;2

Fan J et al (2017) Cloud-resolving model intercomparison of an MC3E squall line case: part I—convective updrafts. J Geophys Res Atmos 122:9351–9378. https://doi.org/10.1002/2017JD026622

Geer AJ et al (2017) The growing impact of satellite observations sensitive to humidity, cloud and precipitation. Q J R Meteorol Soc 143:3189–3206. https://doi.org/10.1002/qj.3172

Guan H, Cui B, Zhu Y, Springs C, I. M. S. Group (2015) Improvement of statistical post-processing using GEFS reforecast information. 841–854, https://doi.org/10.1175/WAF-D-14-00126.1

Guichard F, Couvreux F (2017) A short review of numerical cloud-resolving models. Tellus A Dyn Meteorol Oceanogr 69:1373578. https://doi.org/10.1080/16000870.2017.1373578

Hallegatte S (2012) A cost effective solution to reduce disaster losses in developing countries: hydro-meteorological services, early warning, and evacuation. The World Bank

Holle RL et al (2018) Lightning fatalities and injuries in Bangladesh from 1990 through 2017. In: 25th international lightning detection conference and 7th international lightning meteorology conference, Fort Lauderdale, FL, Vaisala. https://my.vaisala.net/en/events/ildcilmc/archive/Documents/Lightning, Fatalities and Injuries in Bangladesh from 1990 through 2017_R.L. Holle et al.pdf

Holle RL, Dewan A, Said R, Brooks WA, Hossain MF, Rafiuddin M (2019) Fatalities related to lightning occurrence and agriculture in Bangladesh. Int J Disaster Risk Reduct 41: https://doi.org/10.1016/j.ijdrr.2019.101264

Hong S-Y, Lim S (2006) The WRF single-mement microphysics scheme (WSM6). J Korean Meteorol Soc 42:129–151

Hong S-Y, Noh Y, Dudhia J (2006) A new vertical diffusion package with an explicit treatment of entrainment processes. Mon Weather Rev 134:2318–2341. https://doi.org/10.1175/MWR3199.1

Huang X-Y et al (2009) Four-dimensional variational data assimilation for WRF: formulation and preliminary results. Mon Weather Rev 137:299–314. https://doi.org/10.1175/2008MWR2577.1

Janjić ZI (1994) The Step-mountain eta coordinate model: further developments of the convection, viscous sublayer, and turbulence closure schemes. Mon Weather Rev 122:927–945. https://doi.org/10.1175/1520-0493(1994)122%3c0927:TSMECM%3e2.0.CO;2

Jedlovec G (2013) Transitioning research satellite data to the operational weather community: the SPoRT paradigm [organization profiles]. IEEE Geosci Remote Sens Mag 1:62–66. https://doi.org/10.1109/MGRS.2013.2244704

Jirak IL, Melick CJ, Weiss SJ (2014) Combining probabilistic ensemble information from the environment with simulated storm attributes to generate calibrated probabilities of severe weather hazards. In: 27th conference on severe local storms, Madison, Wisconsin, American Meteorological Society, https://ams.confex.com/ams/27SLS/webprogram/Paper254649.html

Kain JS (2004) The Kain-Fritsch convective parameterization: an update. J Appl Meteorol 43:170–181. https://doi.org/10.1175/1520-0450(2004)043%3c0170:TKCPAU%3e2.0.CO;2

Kain JS, Weiss SJ, Levit JJ, Baldwin ME, Bright DR (2006) Examination of convection-allowing configurations of the WRF model for the prediction of severe convective weather: The SPC/NSSL Spring Program 2004. Weather Forecast 21:167–181. https://doi.org/10.1175/WAF906.1

Kain JS et al (2008) Some practical considerations regarding horizontal resolution in the first generation of operational convection-allowing NWP. Weather Forecast 23:931–952. https://doi.org/10.1175/WAF2007106.1

Kain JS, Dembek SR, Weiss SJ, Case JL, Levit JJ, Sobash RA (2010) Extracting unique information from high-resolution forecast models: monitoring selected fields and phenomena every time step. Weather Forecast 25:1536–1542. https://doi.org/10.1175/2010WAF2222430.1

Kathmandu Post (2018) Flood wrecks havoc in Nalgad, Jajarkot. Kathmandu Post

Kotal SD, Bhattacharya SK, Bhowmik SKR, Kundu PK (2015) Development of NWP-based cyclone prediction system for improving cyclone forecast service in the country. High-impact weather events over the SAARC region. Springer, Cham, Switzerland, pp 111–128

Mäkelä A, Shrestha R, Karki R (2014) Thunderstorm characteristics in Nepal during the pre-monsoon season 2012. Atmos Res 137:91–99. https://doi.org/10.1016/j.atmosres.2013.09.012

Mallapaty S (April 2019) Nepali scientists record country's first tornado. Nature

McCaul EW, Goodman SJ, LaCasse KM, Cecil DJ (2009) Forecasting lightning threat using cloud-resolving model simulations. Weather Forecast 24:709–729. https://doi.org/10.1175/2008WAF2222152.1

McCaul EW, Priftis G, Case JL, Chronis T, Gatlin PN, Goodman SJ, Kong F (2020) Sensitivities of the WRF lightning forecasting algorithm to parameterized microphysics and boundary layer schemes. Weather Forecast. WAF-D-19-0101.1, https://doi.org/10.1175/WAF-D-19-0101.1

Milbrandt JA, Yau MK (2006) A multimoment bulk microphysics parameterization. part IV: sensitivity experiments. J Atmos Sci 63:3137–3159. https://doi.org/10.1175/JAS3817.1

Morrison H, Thompson G, Tatarskii V (2009) Impact of cloud microphysics on the development of trailing stratiform precipitation in a simulated squall line: comparison of one- and two-moment schemes. Mon Weather Rev 137:991–1007. https://doi.org/10.1175/2008MWR2556.1

Nakanishi M, Niino H (2009) Development of an improved turbulence closure model for the atmospheric boundary layer. J Meteorol Soc Japan 87:895–912. https://doi.org/10.2151/jmsj.87.895

Nelson EJ et al (2019) Enabling stakeholder decision-making with earth observation and modeling data using tethys platform. Front Environ Sci 7:148. https://doi.org/10.3389/fenvs.2019.00148

NIRAPAD (2018) Monthly hazard incident report, March, April, May. https://www.nirapad.org.bd/home/resources/monthlyHazard

Perrels A (2011) Social economic benefits of enhanced weather services in Nepal

Potvin CK, Flora ML (2015) Sensitivity of idealized supercell simulations to horizontal grid spacing: implications for warn-on-forecast. Mon Weather Rev 143:2998–3024. https://doi.org/10.1175/MWR-D-14-00416.1

Powers JG et al (2017) The weather research and forecasting model: overview, system efforts, and future directions. Bull Am Meteorol Soc 98:1717–1737. https://doi.org/10.1175/BAMS-D-15-00308.1

Rigaud KK (2015) PPCR fundamentals. In: 8th PPCR pilot countries Meeting, Frascati, Italy, Climate Investment Funds, https://www-cif.climateinvestmentfunds.org/sites/default/files/PPCR_Fundamentals_v3_KKR_Final.pdf. Accessed 25 Mar 2016

Roberts B, Jirak IL, Clark AJ, Weiss SJ, Kain JS (2019) Post processing and visualization techniques for convection-allowing ensembles. Bull Am Meteorol Soc 100:1245–1258. https://doi.org/10.1175/BAMS-D-18-0041.1

Romatschke U, Medina S, Houze RA (2010) Regional, seasonal, and diurnal variations of extreme convection in the South Asian region. J Clim 23:419–439. https://doi.org/10.1175/2009JCLI3140.1

Rozumalski RA (2019) UEMS. http://strc.comet.ucar.edu/software/uems/

Schwartz CS, Sobash RA (2017) Generating probabilistic forecasts from convection-allowing ensembles using neighborhood approaches: a review and recommendations. Mon Weather Rev 145:3397–3418. https://doi.org/10.1175/MWR-D-16-0400.1

Schwartz CS, Romine GS, Sobash RA, Fossell KR, Weisman ML (2019) NCAR's real-time convection-allowing ensemble project. Bull Am Meteorol Soc 100:321–343. https://doi.org/10.1175/BAMS-D-17-0297.1

Shrestha A, Pradhananga D, Karmacharya J (2019) Report on Bara-Parsa Tornado, p 82. http://www.smallearth.org.np/wp-content/uploads/2019/04/Report-on-Bara-Parsa-Tornado.pdf

Skofronick-Jackson G, Petersen WA, Berg W, Kidd C, Stocker EF, Kirschbaum DB, Kakar R, Braun SA, Huffman GJ, Iguchi T, Kirstetter PE, Kummerow C, Meneghini R, Oki R, Olson WS, Takayabu YN, Furukawa K, Wilheit T (2017) The global precipitation measurement (GPM) mission for science and society. Bull Am Meteorol Soc 98(8):1679–1695. https://doi.org/10.1175/BAMS-D-15-00306.1

Spencer RW, Howland MR, Santek DA (1987) Severe storm identification with satellite microwave radiometry: an initial investigation with Nimbus-7 SMMR data. J Clim Appl Meteorol 26:749–754. https://doi.org/10.1175/1520-0450(1987)026%3c0749:SSIWSM%3e2.0.CO;2

Stensrud DJ (2007) Parameterization schemes: keys to understanding numerical weather prediction models. Cambridge University Press, Cambridge, p 459

Tao W-K (2007) Cloud resolving modeling. J Meteorol Soc Japan Ser II 85B:305–330. https://doi.org/10.2151/jmsj.85B.305

Tao W-K, Wu D, Lang S, Chern J-D, Peters-Lidard C, Fridlind A, Matsui T (2016) High-resolution NU-WRF simulations of a deep convective-precipitation system during MC3E: Further improvements and comparisons between Goddard microphysics schemes and observations. J Geophys Res Atmos 121:1278–1305. https://doi.org/10.1002/2015JD023986

UCAR (2020) WRF users page. https://www2.mmm.ucar.edu/wrf/users/

Weisman ML, Skamarock WC, Klemp JB (1997) The resolution dependence of explicitly modeled convective systems. Mon Weather Rev 125:527–548. https://doi.org/10.1175/1520-0493(1997)125%3c0527:TRDOEM%3e2.0.CO;2

Williams ER (2001) The electrification of severe storms. In: Severe convective storms, American Meteorological Society, pp 527–561

World Bank (2017) Bangladesh and World Bank sign $113 million to improve weather forecasting and early warning systems. Press Release. http://www.worldbank.org/en/news/press-release/2017/04/05/bangladesh-and-world-bank-sign-113-million-to-improve-weather-forecasting-and-early-warning-systems. Accessed 8 May 2019

World Bank Group—PPCR (2015) Key lessons from the pilot program for climate resilience (Full Report), p 50. https://www-cif.climateinvestmentfunds.org/knowledge-documents/key-lessons-pilot-program-climate-resilience-full-report

Zavodsky BT, LaFontaine FJ, Berndt E, Meyer P, Jedlovec GJ (2017) Satellite data product and data dissemination updates for the SPoRT Sea Surface Temperature composite product. In: 13th symposium new generation operational environmental satellite systems, Seattle, WA, American Meteorological Society, https://ams.confex.com/ams/97Annual/webprogram/Paper315476.html

Zhou L, Lin S-J, Chen J-H, Harris LM, Chen X, Rees SL (2019) Toward convective-scale prediction within the next generation global prediction system. Bull Am Meteorol Soc 100:1225–1243. https://doi.org/10.1175/BAMS-D-17-0246.1

Zhou X, Zhu Y, Hou D, Luo Y, Peng J, Wobus R (2017) Performance of the new NCEP global ensemble forecast system in a parallel experiment. Weather Forecast 32:1989–2004. https://doi.org/10.1175/WAF-D-17-0023.1

Zipser EJ, Liu C, Cecil DJ, Nesbitt SW, Yorty DP (2006) Where are the most intense thunderstorms on earth? Bull Am Meteorol Soc 87:1057–1071. https://doi.org/10.1175/BAMS-87-8-1057